Journal of the Mechanics and Physics of Solids 131 (2019) 43–55

Contents lists available at ScienceDirect

Journal of the Mechanics and Physics of Solids

journal homepage: www.elsevier.com/locate/jmps

Polyacrylamide hydrogels. I. Network imperfection

Canhui Yang[a,c], Tenghao Yin[a,b], Zhigang Suo[a,*]

[a] John A. Paulson School of Engineering and Applied Sciences, Kavli Institute for Bionano Science and Technology, Harvard University, MA 02138, USA
[b] State Key Laboratory of Fluid Power & Mechatronic System, Key Laboratory of Soft Machines and Smart Devices of Zhejiang Province, Center for X-Mechanics, and Department of Engineering Mechanics, Zhejiang University, Hangzhou 310027, China
[c] Department of Mechanics and Aerospace Engineering, Southern University of Science and Technology, Shenzhen, Guangdong 518055, PR China

ARTICLE INFO

Article history:
Received 12 March 2019
Revised 2 June 2019
Accepted 27 June 2019
Available online 27 June 2019

Keyword:
Hydrogel
Polyacrylamide
Rupture
Network imperfection
Fractocohesive length

ABSTRACT

A real polymer network is never perfect, but the quantification of network imperfection has been elusive. Here we quantify the network imperfection of a polyacrylamide hydrogel through its mechanical properties. We find that the ultimate properties—strength, extensibility, and work of fracture—have narrow scatter, comparable to the scatter of modulus. Despite the narrow scatter, the work of fracture is about four orders of magnitude lower than that of the perfect network. This reduction in work of fracture is a measure of network imperfection. The toughness of the hydrogel is about two orders of magnitude higher than that of the perfect network. When the effects of other inelastic processes are minimized, this amplification in toughness is likely due to distributed chain scission, and is another measure of network imperfection. We find that the ultimate properties of the hydrogel are insensitive to cuts up to about 1 mm. We trace this cut insensitivity to network imperfection.

1. Introduction

In an elastomer or a chemical gel, covalent bonds link monomer units into polymer chains, and crosslink polymer chains into a polymer network. The classical theory of entropic elasticity assumes that the polymer network is perfect: all polymer chains have the same length, deform by the same stretch, and break simultaneously; see a review in a recent paper (Mao and Anand, 2018). It is also appreciated that a real polymer network is imperfect. Examples of network imperfection include dangling chains and chains of unequal lengths (Fig. 1). The dangling chains contribute to viscoelasticity, rubbing against the adjacent chains or the solvent (Edwards and Vilgis, 1988). The chains of unequal lengths cause sequential and distributed chain scission (Tehrani and Sarvestani, 2017). Network imperfection affects mechanical properties, such as strength (Bueche, 1959; Tehrani and Sarvestani, 2017) and modulus (Ducrot et al., 2014; Zhong et al., 2016). Network imperfection is also exploited to synthesize tough elastomers (Mark, 2003). Despite decades of efforts, the quantification of network imperfection remains elusive.

Here we study the effects of network imperfection on mechanical properties. We do so by using a polyacrylamide hydrogel as a model material. Polyacrylamide hydrogels are routinely synthesized in many laboratories by free radical polymerization (Caulfield et al., 2002) (Fig. 2). A polyacrylamide hydrogel consists of a covalent polymer network and water. The molar

---

[*] Corresponding author.
E-mail address: suo@seas.harvard.edu (Z. Suo).

https://doi.org/10.1016/j.jmps.2019.06.018
0022-5096/© 2019 Published by Elsevier Ltd.

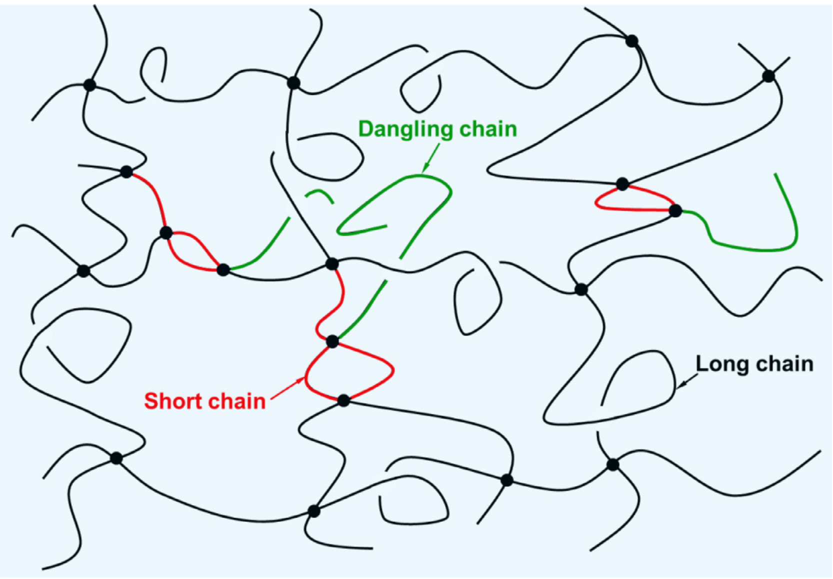

Fig. 1. A real polymer network is imperfect. Coexistent in the network are long chains, short chains, and dangling chains.

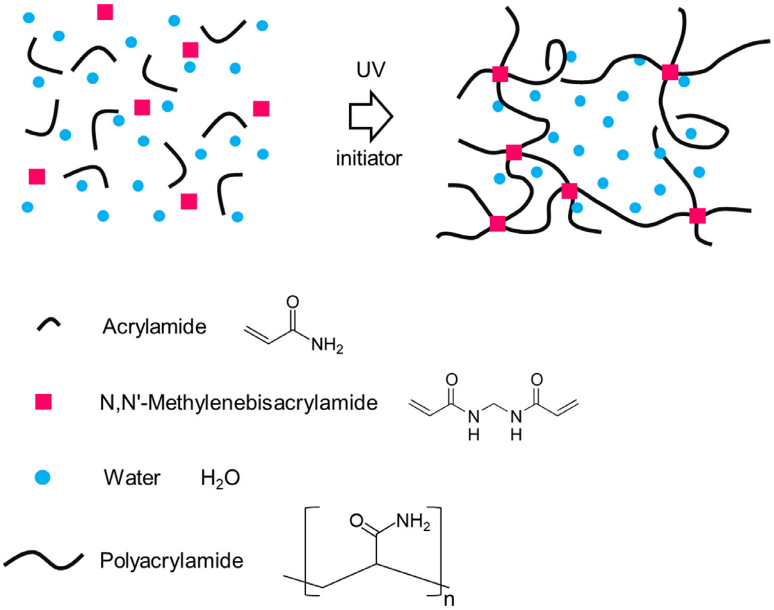

Fig. 2. Synthesis of a polyacrylamide hydrogel. The precursor is a mixture of the monomer (acrylamide), the crosslinker (N'N-Methylenebisacrylamide), the initiator, and water. A UV light triggers free radical polymerization, leading to a hydrogel. Covalent bonds link the monomer units into polymer chains, and crosslink the polymer chains into a polymer network. Water molecules are mobile in the polymer network.

ratio of the monomer to the crosslinker ranges from 10 to 10^4. The volume fraction of water varies from 70% to 90%. Under ordinary conditions, the polyacrylamide network is stable, and water is mobile in the polymer network. Polyacrylamide hydrogels have broad and well-established applications in biology, agriculture, and medicine, so that many chemical and biological properties have been characterized (Caulfield et al., 2002). The mechanical properties of polyacrylamide hydrogels have been reviewed recently (Bai et al., 2019b). It appears that polyacrylamide is a hydrogel of choice in developing new concepts. Polyacrylamide is the primary network in many tough hydrogels (Gong et al., 2003; Sun et al., 2012). Polyacrylamide hydrogels containing salts are used as stretchable, transparent, ionic conductors in ionotronics (Keplinger et al., 2013; Lee et al., 2018; Yang and Suo, 2018). Polyacrylamide hydrogels have been used as a model material to study the growth of cracks in hydrogels under static (Tanaka et al., 2000), cyclic (Tang et al., 2017), and dynamic (Kolvin et al., 2018) loads.

Just as silica has long served as a model hard material (Griffith, 1921), we now use a polyacrylamide hydrogel as a model soft material. Both materials are highly elastic prior to rupture, but some differences are puzzling. Whereas the strength of silica scatters enormously, often by orders of magnitude (Proctor et al., 1967), the strength of a polyacrylamide hydrogel scatters narrowly, typically less than 10% (e.g., see data presented in this paper). For silica, the scatter in strength is much larger than that in modulus. For the polyacrylamide hydrogel, however, the scatter in strength is comparable to that in modulus. The large scatter in strength of silica is known to be caused by crack-like flaws, but what makes the scatter in strength of the hydrogel so narrow? Furthermore, the strength of the polyacrylamide hydrogel remains nearly constant even when a sample is cut with a crack prior to the tensile test, so long as the cut is shorter than a certain length, about 1 mm. That polyacrylamide hydrogel is cut-insensitive was noted in a previous paper focused on elastomers (Chen et al., 2017). It was also noted that this “certain length” is much larger than the mesh size of the hydrogel. But where does this certain length come from?

We hypothesize that network imperfection profoundly affects mechanical properties. Just as we characterize a thermodynamic state through measurable properties like temperature, pressure, volume, energy, and entropy, we characterize network imperfection through measurable properties like modulus, strength, extensibility, work of fracture, and toughness. Indeed, mechanical properties provide quantitative measures of network imperfection once we minimize effects such as viscoelasticity, crystallization, and fillers, which confound the analysis of the mechanical properties of elastomers. Because polyacrylamide chains are typically long and water has low viscosity, a polyacrylamide hydrogel of high water content is highly stretchable, but negligibly viscous. The hydrogel has no fillers and does not crystalize. This combination of attributes simplifies analysis, and is essential to our use of the polyacrylamide hydrogel to study network imperfection. Indeed, solvents have been used to swell elastomers to minimize the effect of viscoelasticity in the study of fracture (Ahagon and Gent, 1975). In general, viscoelasticity, crystallization, and fillers in elastomers do profoundly affect strength (Hamed, 2007; Smith, 1978) and toughness (Gent, 1996; Greensmith, 1956). These confounding effects mask something basic: network imperfection also profoundly affects mechanical properties.

We ascertain the hypothesis by synthesizing polyacrylamide hydrogels and measuring their mechanical properties (Section 2), as well as by comparing the measured mechanical properties of the hydrogel to the theoretical values of a perfect network. Our experiments show that the ultimate properties (strength, extensibility, and work of fracture) have narrow scatter, comparable to the scatter of the modulus (Section 3). Despite the narrow scatter, the work of fracture of hydrogel is lower than that of a perfect network by about four orders of magnitude. This reduction in work of fracture is a measure of network imperfection. The hydrogel exhibits a small but measurable Mullins effect (Section 4). In the absence of fillers, the Mullins effect indicates sequential and distributed chain scission due to network imperfection. The toughness of the hydrogel is higher than that of a perfect network by two orders of magnitude (Section 5). This amplification in toughness is likely due to the distributed chain scission, and is another measure of network imperfection. Distributed chain scission acts as a solid-like toughener, amplifies the threshold for the growth of a crack under static load, but not the threshold for the growth a crack under cyclic load (Section 6). The ratio of the toughness (measured by rupturing samples of long cuts) to the work of fracture (measured by rupturing samples of no cuts) defines a material specific length, which we call the fractocohesive length. Our experiments confirm that a cut shorter than the fractocohesive length has negligible effects on the ultimate properties of the hydrogel (Section 7). The fractocohesive length is on the order of 1 mm for the hydrogels in this work, whereas the fractocohesive length is on the order of the mesh size of the network for a perfect network. For the hydrogel, it is the network imperfection that causes cut insensitivity. These experimental measurements map network imperfection to mechanical properties.

2. Chemical synthesis and mechanical tests

We purchase acrylamide (AAm, A8887), N,N’-Methylenebisacrylamide (MBAA, M7279), 2-Hydroxy-4′-(2-hydroxyethoxy)–2-methylpropiophenone (Irgacure 2959, 410896), and pure ethyl alcohol (CH_3CH_2OH, 459844) from Sigma Aldrich. We purchase glass sheets and Perspex sheets from McMaster-Carr.

We dissolve 14 g of the acrylamide monomer and 0.0085 g of the crosslinker MBAA in 86 g of deionized water. (The molar ratio of acrylamide to MBAA is 3572.) We dissolve the photo-initiator Irgacure 2959 in ethyl alcohol to form a solution of concentration 0.1 M. For every 1 ml of the aqueous solution of the monomer and crosslinker, 1.5 µl of the solution of initiator is added. The resulting mixture is poured into a glass mold, and cured with a UV light (15 W, 365 nm, UVP XX-15 L) for 75 min. During the curing process, the acrylamide monomers form polyacrylamide chains and the polyacrylamide chains are crosslinked by the crosslinkers to form a network (Fig. 2). The curing process is a free radical polymerization. The randomness of free radical polymerization leads to a polyacrylamide network of uneven chain lengths. After the curing, we disassemble the glass mold and obtain the polyacrylamide hydrogel.

We glue the polyacrylamide hydrogels onto Perspex sheets. The samples of the hydrogel are 1.5 mm thick, 6 cm long, and 1 cm high. Some samples are not cut with cracks, but others are cut with cracks of various lengths. A razor blade is used to make an edge cut in the middle line of the sample. For the cut longer than 1 mm, a ruler is used to measure its length. For the cut shorter than 1 mm, the length is measured under a microscope. We then load the samples on a mechanical testing machine (Instron 5966).

3. Stress–stretch curves

Mechanical properties of hydrogels are often viscoelastic and poroelastic. Here we minimize these inelastic effects to let network imperfection stand out. In conducting mechanical tests, we select a time window, within which viscoelastic

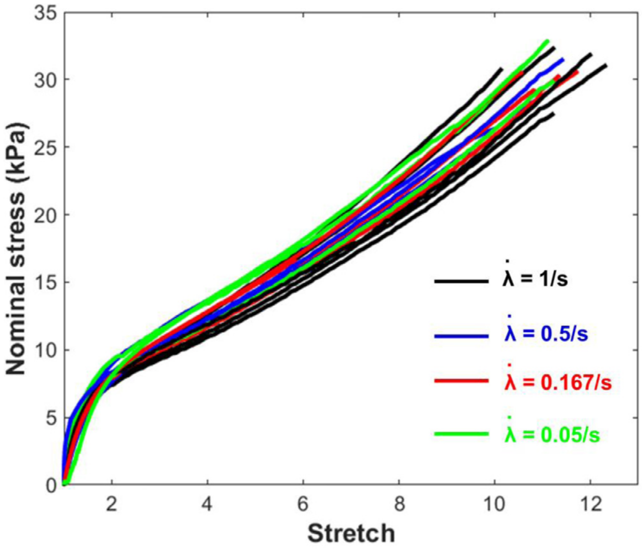

Fig. 3. Stress-stretch curves up to rupture, obtained using 14 samples at four rates of stretch.

relaxation has completed and poroelastic relaxation barely starts. We use four rates of stretch: 0.05/s, 0.167/s, 0.5/s, and 1/s. Given the total stretch on the order of 10, the total time of each experiment ranges from 10 to 200 s. Viscoelastic relaxation time for polyacrylamide hydrogel is on the order of 1 s (Hu and Suo, 2012; Tian et al., 2018), much shorter than the experimental time scale in this work. The relevant length for poroelasticity is the thickness of the specimen, $B = 1.5$ mm. The effective diffusivity of water molecule in a polyacrylamide hydrogel is on the order of $D \sim 10^{-10}$ m^2/s (Kalcioglu et al., 2012), the time needed for poroelasticity to prevail is on the order of $B^2/D \sim 10^4$ s, which is much longer than the experimental time scale in this work. We conduct experiments in open air. When the rate of stretch is low, the total experimental time becomes long and the loss of water cannot be neglected. For example, at the rate of stretch 0.0167/s, the experimental time is up to ~10 min, and we record more than 18% of loss of mass. The loss of mass is below 3.5% when the rate of stretch is 0.05/s.

Within the range of loading rate, all stress–stretch curves are similar: the scatter among samples tested with different loading rates is comparable to that among samples tested with the same loading rate (Fig. 3). We will not study the effect of loading rate any further in this paper. The stress–stretch curves give the following average values of the mechanical properties: 1.9×10^5 J/m^3 for the work of fracture (i.e., the area beneath the stress–stretch curve), 11.1 for the extensibility, 30.5 kPa for the strength, and 4.6 kPa for the shear modulus. For each of the four quantities, the standard deviation normalized by the average is 6.7%, 4.5%, 3.3%, 5.3%, respectively. The ultimate properties and the shear modulus have similar statistical scatter. Similarly small scatter in the ultimate properties has been noted for elastomers (Smith, 1978). By contrast, brittle hard materials such as silica often have little statistical scatter in modulus, but enormous statistical scatter in the ultimate properties (Griffith, 1921; Proctor et al., 1967). It is this stark contrast between the hydrogel and silica that initially drew our attention, which has led to this series of study. Why is the scatter in the ultimate properties of the hydrogel so narrow?

In the above, the shear modulus of each sample is calculated by fitting the initial portion of the experimentally measured stress–stretch curve to the Neo-Hookean model. The model assumes the Helmholtz function

$$W = \frac{1}{2}\mu\left(\lambda_1^2 + \lambda_2^2 + \lambda_3^2 - 3\right),$$

where μ is the shear modulus, and λ_1, λ_2, λ_3 are principal stretches. The sample of the hydrogel has a long rectangular shape. The clamps constrain the deformation in the horizontal direction, so that $\lambda_1 = 1$. The hydrogel is taken to be incompressible, $\lambda_1 = 1/\lambda_2$. The Helmholtz function is reduced to

$$W = \frac{1}{2}\mu\left(\lambda_2^2 + \lambda_2^{-2} - 2\right).$$

The nominal stress is calculated from $s_2 = dW/d\lambda_2$, giving

$$s_2 = \mu\left(\lambda_2 - \lambda_2^{-3}\right).$$

When deformation is small, $\lambda_2 \to 1$, the stress–stretch curve is linear,

$$s_2 = 4\mu(\lambda_2 - 1).$$

The initial slope of the stress–stress curve is four times the shear modulus. This linear equation is used to fit the initial slope of each measured stress–stretch curve to obtain the shear modulus.

Despite the narrow scatter, the ultimate properties of the hydrogel are far below those of a perfect network. In a perfect network, all polymer chains have the same number of monomers, deform by the same stretch, and break simultaneously. For example, the eight-chain model is a perfect network (Arruda and Boyce, 1993). Here we estimate the work of fracture of a perfect network by the density of covalent energy:

$$W_{th} = \phi J/V,$$

where ϕ is the volume fraction of polymer in the hydrogel, J is the covalent energy per bond along a polymer chain, and V is the volume per monomer. For the polyacrylamide hydrogel, the volume fraction of polymer is about $\phi \sim 12.8\%$, the covalent energy of a C–C bond is $J \sim 5 \times 10^{-19}$ J (Luo, 2007), and the volume per monomer is on the order of $V \sim 10^{-28}$ m^3, the density of covalent energy of a perfect network is estimated as $W_{th} \sim 6.4 \times 10^8$ J/m^3, which is much higher than the measured work of fracture of the hydrogel (1.9×10^5 J/m^3). Similar values of work of fracture are measured for other hydrogels in which the polyacrylamide is used as covalent networks (Nakajima et al., 2012; Sato et al., 2015; Sun et al., 2012; Yang et al., 2013). For unfilled, but crosslinked, natural rubber, the measured work of fracture is on the order of 10^7 J/m^3 (Greensmith, 1960; Thomas, 1955, 1958), which is much lower than the covalent energy of a perfect network ($\sim 10^{10}$ J/m^3). The measured strength is also much lower than that of a perfect network as well. The rupture force of a C–C bond is a few nN, e.g. 2 nN (Beyer, 2000), and the area per monomer is 2.2×10^{-19} m^2, giving the theoretical strength of C–C bond of 9×10^9 Pa. In a perfect network, every bond carries the same load, so that the strength of network is same as that of the bond. Further taking the volume fraction of polymer, 12.8%, into account, the theoretical strength of a perfect network is estimated to be on the order of 10^9 Pa. By contrast, the measured strength of the polyacrylamide hydrogel is on the order of 10^4 Pa.

Large discrepancy between the theoretical and experimental values of work of fracture is common to most materials. The low experimental strength of brittle rigid materials like silica is due to crack-like flaws (Griffith, 1921). By contrast, we will show later that small crack-like flaws do not affect the strength of the hydrogel. We surmise that the reduction in the work of fracture of the hydrogel is due to network imperfection, such as dangling chains and chains of unequal lengths. We regard the reduction in the work of fracture as a measure of network imperfection.

The measured extensibility is also lower than that of a perfect network. For a polymer chain in a perfect network, assume that the polymer chain has n repeats of monomers, and the length per monomer is a. In the undeformed state, the distance between the two ends of the polymer chain is $\sqrt{n}a$, determined by the random-walk model. In the state right before rupture, the polymer chain is fully extended and its length becomes na. The ratio of the two lengths gives the theoretical extensibility, $\sqrt{n}$. We calculate n for a perfect network as follows. Assume that all the acrylamide monomers and MBAA crosslinkers are polymerized into the network. In the perfect network, each crosslinker connects to four polymer chains, each polymer chain connects to two crosslinkers, and each polymer chain has n monomers. Consequently, n is one half of the molar ratio of the monomer to the crosslinker. We have synthesized the hydrogels using the molar ratio of 3572, so that the perfect network has $n = 1786$ monomers. Thus, the extensibility of a perfect network is about 42, much larger than the measured extensibility ($\sim$11). The above theoretical estimate can be refined. For example, the monomer units are not freely jointed, which reduces the extensibility (Dobrynin et al., 2004). Also, before scission, the length of each individual covalent bond is stretched, which increases the extensibility (Mao and Anand, 2018). The chains rotate during deformation (Arruda and Boyce, 1993). Here we do not pursue these refinements.

Unlike the ultimate properties, the modulus is close between theoretical limits and experimental measurements. The theoretical shear modulus is estimated by $\mu_{th} = \phi_p^{1/3} NkT$ (Cai and Suo, 2012), where N is the number of polymer chains per unit volume of the dry polymer, $Kt = 4.1 \times 10^{-21}$ J is the temperature in the unit of energy, and ϕ_p is the volume fraction of polymer in the hydrogel. For the hydrogel in our experiment, the volume fraction of polymer network is $\phi_p = 12.8\%$. For a perfect network, $N = 1/(nV)$, where $n = 1786$ is the number of monomers per polymer chain, and V is the volume per monomer. For acrylamide, the mass per molecule is 1.2×10^{-22} g, the density 1.13 g/cm^3, and their ratio gives $V = 10^{-28}$m^3. These values give the theoretical shear modulus, $\mu_{th} = 11.5$ kPa. The experimentally measured shear modulus is 4.6 kPa. The difference between estimation and measurement may originate from theoretical refinements and experimental errors. For example, the theoretical estimation assumes that all polymer chains carry load and contribute to shear modulus. However, in a real network, only the crosslinked polymer chains contribute to shear modulus, other chains such as dangling chains do not. The number of chains in a real network is less than that in a perfect network, due to the incomplete conversion from monomers into polymers. Experimental errors include the initial balance setting of tests, dimension measurement of the samples and numerical fitting in the initial slop of stress–stretch curves, etc.

4. Mullins effect

It is often assumed that a polyacrylamide hydrogel has near-perfect elasticity. This ideal picture is inconsistent with a real network with imperfection. As the hydrogel is stretched, some polymer chains break before others. The intact chains stabilize the damaged network, so that broken chains distribute throughout the network. The sequential and distributed scission of chains is an inelastic process, which we now quantify by the Mullins effect (Mullins, 1948). We load, unload, and reload a hydrogel to a sequence of maximum stretches (Fig. 4). When the stretch is less than the previous stretch, the reloading curve is below the previous loading curve. When the stretch is larger than the previous stretch, the stress–stretch curve is approximately the same as if the sample has not been previously stretched. The area under a loading curve

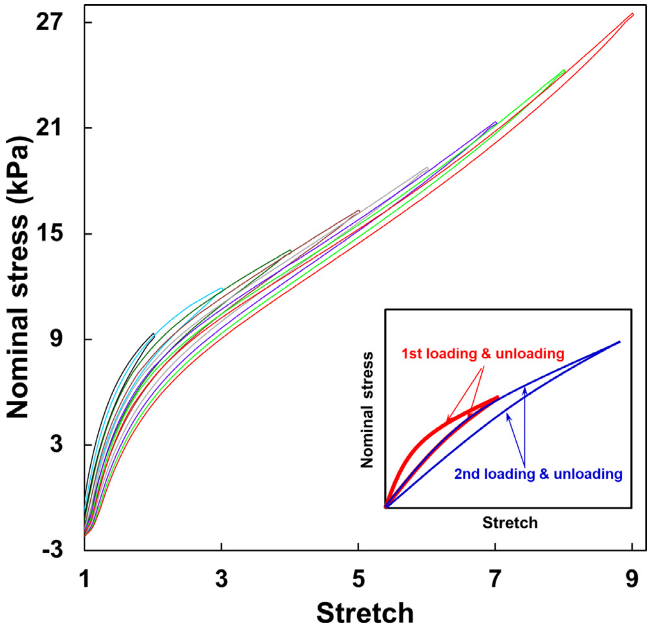

Fig. 4. Mullins effect. Nominal stress-stretch curves of a hydrogel subject to a sequence of loading and unloading with increasing maximum stretch before unloading. The inset shows loading and unloading curves of ideal Mullins effect.

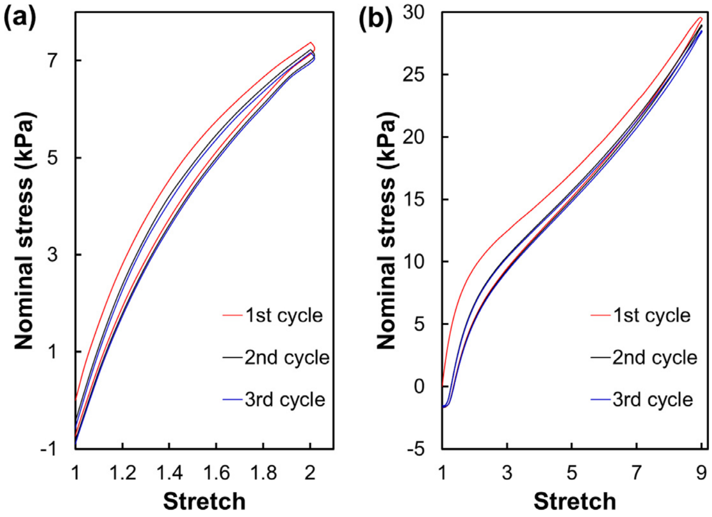

Fig. 5. Dissipation reduction. Cyclic loading and unloading with fixed maximum stretch of 2, (a), and 9, (b), before unloading.

is the work done by the load. The area between a loading and an unloading curve is the energy dissipated during the load and unload. One may define hysteresis by the ratio of the energy dissipated to the work done (Wang et al., 2019). Hysteresis so defined is a number between 0 and 1. For the sample under a sequence of load, unload, and reload (Fig. 4), the hysteresis is 0.14, 0.13, 0.1, 0.08, 0.07, 0.06, 0.06, and 0.05 at the maximum stretches of 2, 3, 4, 5, 6, 7, 8, 9. In the absence of other confounding effects (e.g., poroelasticity, viscoelasticity, and fillers), we regard the hysteresis as a measure of network imperfection of the polyacrylamide hydrogel. We note that the nominal stress at stretch of 1 after unloading is negative, which is mainly ascribed to the residual deformation caused by distributed chain scission.

We also cyclically load two fresh samples (Fig. 5). For the sample subject to a maximum stretch of 2, the first three cycles dissipate energy by 0.55 kJ/m^3, 0.34 kJ/m^3, and 0.31 kJ/m^3. For the sample subject to a maximum stretch of 9, the first three cycles dissipates energy by 17.77 kJ/m^3, 5.4 kJ/m^3, and 5.55 kJ/m^3. A larger stretch damages the network more, and dissipates more energy. Chain scission is an irreversible process. After scission, a polymer chain breaks into two dangling polymer chains. As a result, the chain scission only contributes to energy dissipation for the first loading cycle. We attribute the difference in the energy dissipated in the first and the second loading cycle to distributed chain scission. From the second

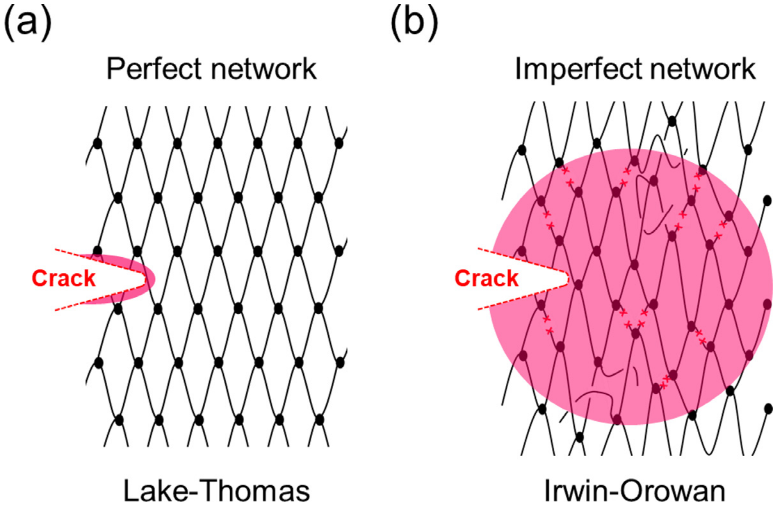

Fig. 6. Lake–Thomas vs Irwin–Orowan. (a) A perfect network undergoes affine deformation that all chains deform the same. Upon fracture, all chains break simultaneously. A perfect network fractures by the Lake-Thomas picture. (b) An imperfect network undergoes nonaffine deformation. Upon fracture, the short chains break before the long chains. The rupture of short chains dissipates energy over a large volume of network off the plane of the crack. An imperfect network fractures by the Irwin–Orowan picture.

loading cycle on, each cycle dissipates a similar amount of energy. Such hysteresis loops persist in polyacrylamide hydrogels even after thousands of cycles (Bai et al., 2017). The molecular origin of this narrow, but persistent, hysteresis has not been studied.

It is curious that the Mullins effect has not been reported for unfilled, noncrystalizing elastomers (Diani et al., 2009). The Mullins effect has been studied for a double-network hydrogel, where one network has short chains and the other network has long chains (Webber et al., 2007). When the hydrogel is stretched, the short-chain network breaks, but the long-chain network remains intact.

5. Toughness

Toughness of a material is the energy dissipated in advancing a crack in the material by a unit area. In a perfect polymer network, a crack advances by breaking a single layer of polymer chains on the crack plane, while all polymer chains off the crack plane remain intact (Fig. 6a). The picture gives a theoretical estimate of the toughness (Lake and Thomas, 1967):

$$\Gamma_{th} = \phi\sqrt{n}aJ/V$$

Lake and Thomas originally proposed the model for elastomers. Just before a polymer chain breaks, the entire chain is stretched taut, so that every covalent bond in the chain is stretched near the covalent energy. When the chain breaks, the entire chain retracts, and dissipates the energy stored in the chain. The product aJ/V is the same for any solid, such as silica. The Lake-Thomas model shows that the polymer chain amplifies the toughness by a factor of $\sqrt{n}$. The above equation has been modified to include the effect of the volume fraction of polymer in the hydrogel, ϕ. The Lake-Thomas model is a scaling analysis, so that a numerical factor of order unity is undetermined, and is dropped from the above equation (Bai et al., 2018). With values $\phi = 12.8\%$, $V = 10^{-28}$ m^3, $J = 5 \times 10^{-19}$ J, $a = 4.6 \times 10^{-10}$ m, and $n = 1786$, we estimate that $\Gamma_{th} = 12.4$ J/m^2.

An imperfect network contains polymer chains of distributed lengths. Before a long polymer chain at the crack front breaks, the network transmits the high stress from the crack front into the network. In the network, off the crack plane, some short chains break, while long chains remain intact (Fig. 6b). Consequently, as the crack advances in the imperfect network, energy dissipates to break not only a layer of polymer chains on the crack plane, but also some short chains off the crack plane. This synergy of molecular cleavage and bulk hysteresis is common in most tough materials, as captured in the Irwin–Orowan picture (Irwin, 1948; Orowan, 1950). Background hysteresis has been exploited in developing tough elastomers (Ducrot et al., 2014; Hamed, 1994; Llorente et al., 1981; Mark, 1994) and tough hydrogels (Gong et al., 2003; Sun et al., 2012).

We measure the toughness by using samples with edge cracks (Fig. 7a). A sheet of the hydrogel, of dimensions H in height, B in thickness and T in width, is fastened by rigid clamps. Prior to stretch, a cut of length c is made at the edge of the sample. Then the sample is pulled from the original height H to the height λH (Fig. 7b). Thus the stretch of the sample is λ. We use a razor blade to make cut and mark the cut using a blue dye (Fig. 7c). When the sample is stretched, the cut blunts (Fig. 7d). We vary the length of the cut. For a cut of length below 1 mm, the length of the cut is measured under a microscope (Fig. 7e). We use a high stretch rate of 1/s so that poroelastic relaxation is insignificant.

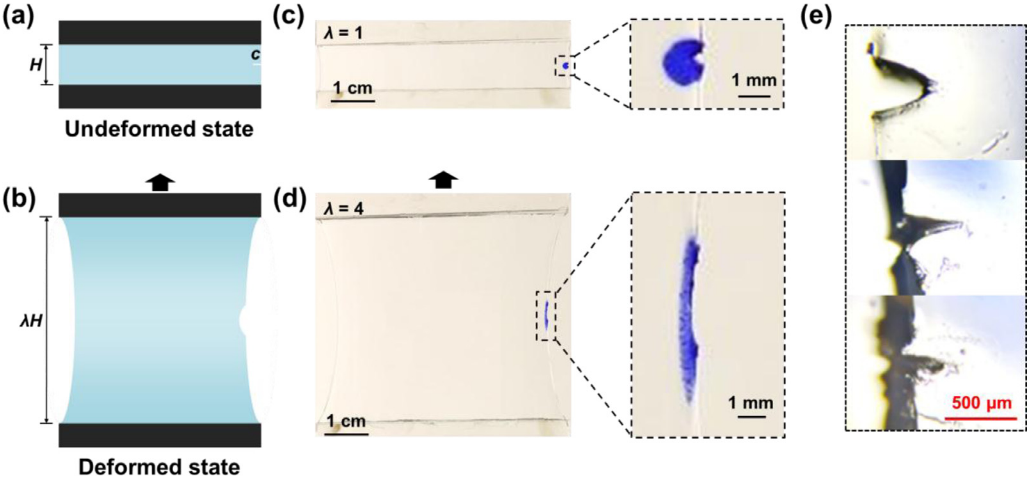

Fig. 7. Experimental setup to measure the effects of cut on rupture. (a) In the undeformed state, a rectangular-shaped sample of dimensions H in height, B in thickness and T in width is fastened to rigid clamps. A crack is cut at one edge of the sample with depth c. (b) When the sample is stretched, the distance between the two rigid clamps becomes λH. (c) A polyacrylamide hydrogel is clamped by two acrylic sheets. In the undeformed state, the height of the hydrogel is 1 cm, thickness is 1.5 mm, and width is 6 cm. A small crack is cut at right edge of the hydrogels by using a razor blade. The crack is dyed blue. The right image shows the magnified crack. (d) The polyacrylamide hydrogel is stretched to 4 times its original height. The right image shows that the cut blunts. (e) For a cut of length below 1 mm, the length is measured under a microscope. Three samples with cuts of different lengths are shown.

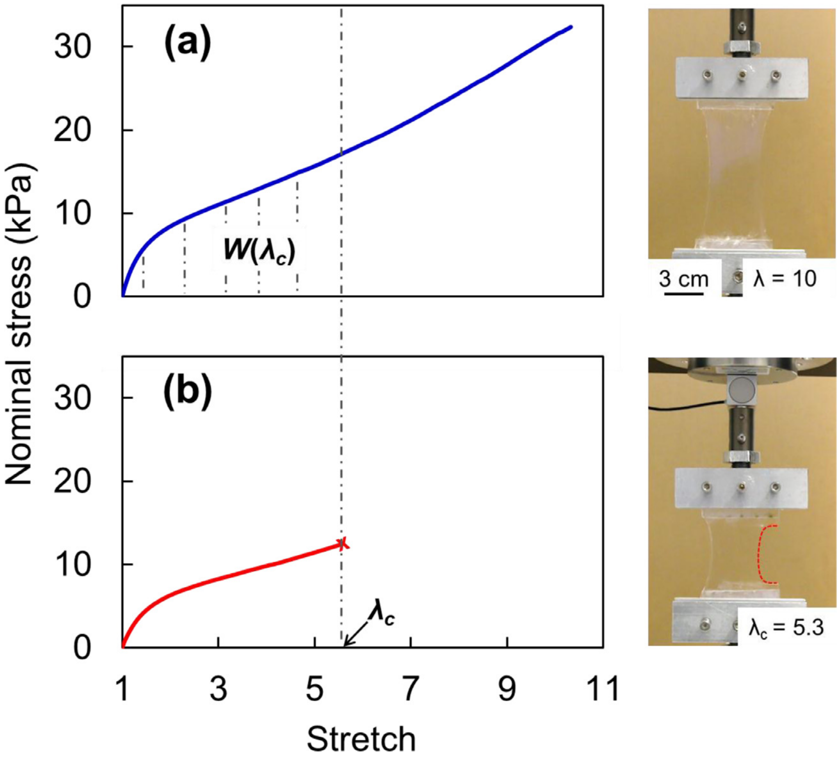

Fig. 8. Experimental measurement of toughness. (a) Nominal stress-stretch curve of a sample without cut. The right image shows the sample under a stretch of 10, close to rupture. (b) Nominal stress-stretch curve of a sample with a cut of length 1 cm. The sample ruptures at a critical stretch $\lambda_c = 5.3$. The energy density at critical stretch is obtained from the nominal stress–stretch curve of the sample without cut, $W(\lambda_c)$. The right image shows the sample at the critical stretch.

We firstly load one sample without cut all the way to rupture and obtain the nominal stress–stretch curve (Fig. 8a). Then we load another sample with a cut of length 1 cm and record the nominal stress–stretch curve until the onset of crack propagation at a critical stretch λ_c (Fig. 8b). The total energy U stored in the sample at the critical stretch is $W(\lambda_c)\cdot B\cdot T\cdot H$, where $W(\lambda_c)$ is the energy density, calculated as the area under the nominal stress–stretch curve of the sample without cut at λ_c. The toughness is the energy needed to advance the crack by unit area and can be calculated from (Rivlin and Thomas, 1953; Sun et al., 2012),

$$\Gamma = W(\lambda_c)\cdot H$$

The above equation gives $\Gamma = 515.7 \pm 19.4\,\mathrm{J/m^2}$.

The toughness determined here is comparable with values previously reported for polyacrylamide hydrogels, typically in the range 100–1000 $\mathrm{J/m^2}$ (Bai et al., 2018; Sun et al., 2012). The toughness of polyacrylamide hydrogels depends on crosslink density and water content (Zhang et al., 2018). Different methods of measurement may also affect the values. For example, relative to the plane normal to the crack front, the peel test satisfies the plane strain condition while the pure shear test satisfies the plane stress condition. It is conceivable that the toughness measured by the peel test differs from that measured by the pure shear test, although such difference has not been studied for hydrogels.

These details, however, do not affect a basic fact: the toughness of polyacrylamide hydrogels reported here and elsewhere are much higher than the Lake-Thomas prediction for a perfect network. The toughness of the hydrogel is about two orders of magnitude higher than that of a perfect network. This amplification in toughness is due to background hysteresis. As our measurement of the Mullins effect has indicated, a main contributor to hysteresis is the distributed chain scission due to network imperfection. We regard the amplification in toughness as another measure of network imperfection.

6. Fatigue cracks under prolonged static and cyclic loads

Fatigue of hydrogels has been reviewed recently (Bai et al., 2019a). Here we do not report any new experiments on fatigue, but wish to note that distributed chain scission may explain certain puzzling observations reported before.

Tang et al. (2017) discovered that polyacrylamide hydrogels suffer crack growth under cyclic load when the energy release rate is much below the toughness, but is above a threshold. The measured threshold is comparable to the Lake-Thomas prediction. These findings have been confirmed in subsequent experiments on cyclic fatigue of polyacrylamide hydrogels (Bai et al., 2018; Zhang et al., 2018), but the molecular mechanism for cyclic fatigue crack growth in polyacrylamide hydrogels has yet been identified (Bai et al., 2019a). How does a material of near-perfect elasticity fatigue? Here we surmise that network imperfection is a mechanism for cyclic fatigue crack growth in polyacrylamide hydrogels. The polyacrylamide hydrogel is not elastic enough: the narrow, but measurable, Mullins effect indicates distributed chain scission due to network imperfection. When a crack advances in the hydrogel under monotonic load, the bulk hysteresis amplifies the toughness of the hydrogel from that of a perfect network. When a crack advances in the hydrogel under a cyclic load, however, previous cycles cause distributed chain scission, which becomes unavailable to enhance the threshold.

Tang et al. (2017) also discovered that the threshold for delayed fracture is above the threshold for cyclic fatigue crack. The difference between the two thresholds is understood by introducing the concept of solid-like tougheners (Bai et al., 2019a). Here we surmise that distributed chain scission acts as a solid-like toughener. The hysteresis due to distributed chain scission is insensitive to loading rate. Such hysteresis amplifies the threshold for crack growth under a static load, but contributes negligibly to threshold for crack growth under cyclic load.

7. Cut sensitivity and fractocohesive length

We next show another consequence of network imperfection: lower cut sensitivity. We measure the ultimate properties of the polyacrylamide hydrogels that contain cuts of various lengths (Fig. 9). Even without the intentional cut, crack-like defects are inevitable during the synthesis of the hydrogels, but these defects are hard to observe. To represent the uncertainty in the lengths of crack-like defects associated with synthesis, we draw horizontal lines from the mesh size to 10^{-4} m. For the precut samples, we manually make the cut and measure the length. Experimental data show that the ultimate properties of uncut samples have the comparable scatter as those of precut samples. There is a critical length of cut, below which the ultimate properties are insensitive to the length of cut and similar to that of uncut samples. For the polyacrylamide hydrogel, this critical length of cut is on the order of 10^{-3} m.

The cut-sensitivity diagram (Fig. 9a) is understood as follows (Chen et al., 2017). Three length scales are involved: the length of the cut c; the size of the sample, here represented by the height H; and a material-specific length Γ/W_f, which we propose to call fractocohesive length. The fractocohesive length is the ratio of two mechanical properties: the toughness Γ, which has the dimension of energy per unit area, and is measured using a sample containing a long crack; and the work of fracture W_f, which has the dimension of energy per unit volume, and is measured using a sample containing no precut crack.

For a long cut in a large sample, when the sample is stretched to advance the cut, only a small zone around the cut tip is inelastic. Outside the inelastic zone, the sample is elastic; see a recent review on crack-tip field (Long and Hui, 2015). The field equations of elasticity do not contain any length scale, nor do the boundary conditions of a long crack in a large

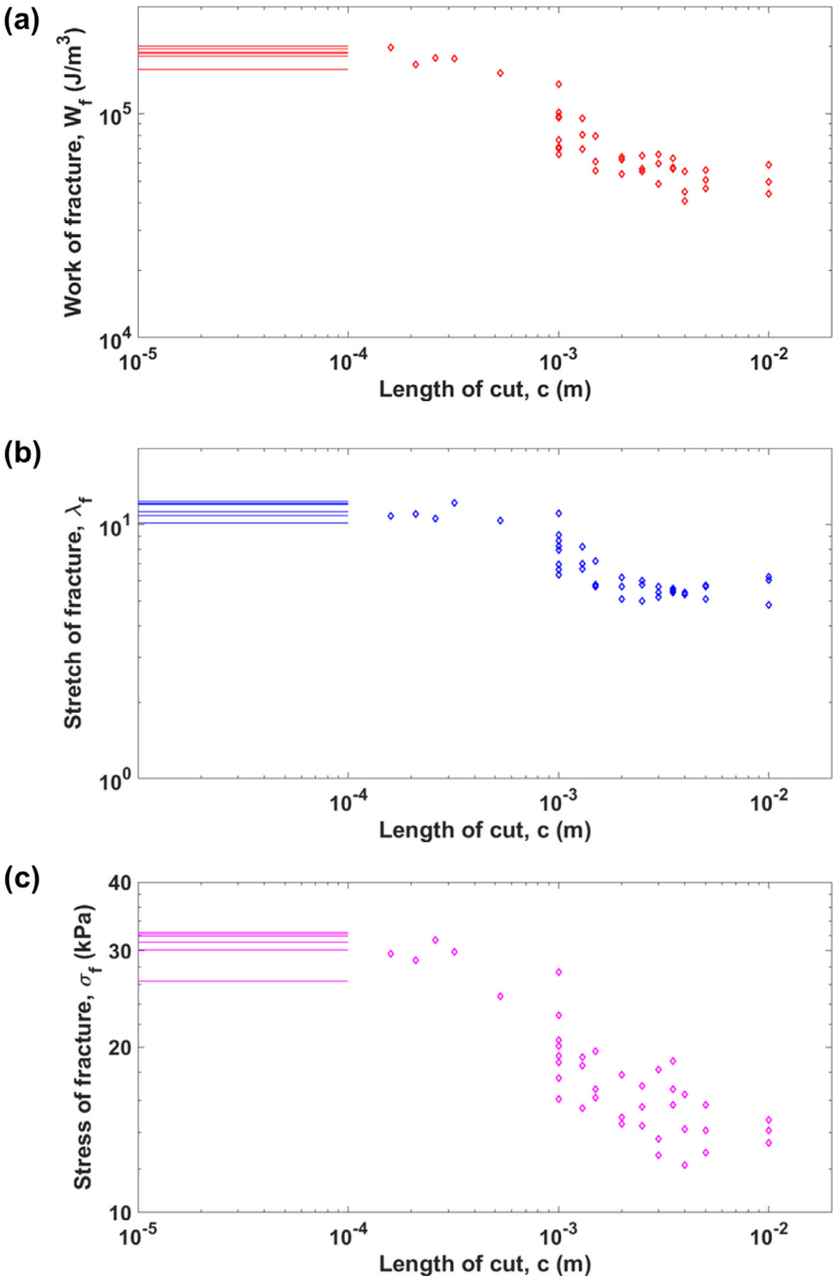

Fig. 9. Effects of cuts on the ultimate properties. (a) Work of fracture W_f, (b) extensibility (i.e. stretch of fracture) λ_f, and (c) strength (i.e. stress of fracture) σ_f as a function of the length of cut. Solid lines represent the ultimate properties measured using samples without cut. The lines vary over a range below 10^{-4} m, indicating that we are uncertain about the length of crack-like cuts associated with synthesis. The data points are measured using samples with cut.

sample. Recall that the Helmholtz function has the unit of energy per volume, and the toughness has the unit of energy per area. Consequently, the field of the Helmholtz function scales as

$$W \sim \frac{\Gamma}{2\pi R},$$

where R is the distance of a material particle in the sample to the tip of the cut, measured when the sample is in the undeformed state. The dimensionless pre-factor, of order unity, depends on the polar angle and the dimensionless parameters in the model of elasticity (if any), and is independent of inelasticity. The fracture process, however complex, affects this elastic field through a single parameter: the toughness Γ. Indeed, toughness Γ is experimentally determined using a large sample containing a long cut.

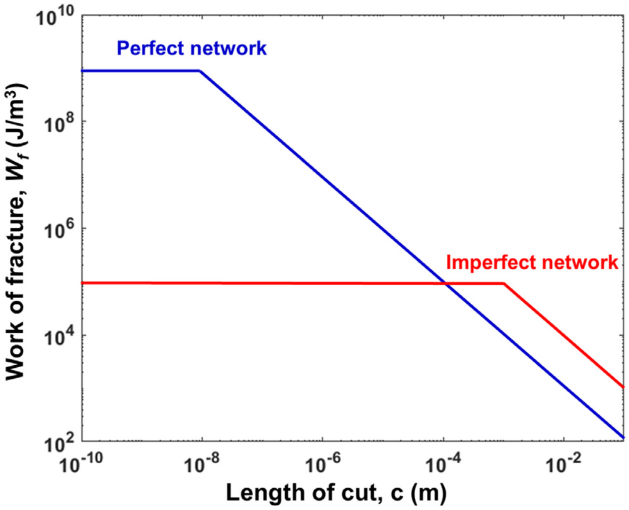

Fig. 10. Cut sensitivity diagram. The work of fracture is cut-insensitive when the cut is short, but is cut-sensitive when cut is long. The transition occurs at about 10 nm for a perfect network, and about 1 mm for a real, imperfect network.

The above elastic field is valid in an annulus, of the inner radius larger than the inelastic zone and outer radius smaller than the sample size. Setting W to the work of fracture, the above equation estimates the size of inelastic zone:

$$R_1 \sim \frac{\Gamma}{2\pi W_f}$$

The size of the inelastic zone scales with the fractocohesive length. When the size of the inelastic zone is small compared with the length of the cut, $R_I < c$, the condition of small-scale inelasticity prevails, and the work of fracture is inversely proportional to the length of the cut. When the size of the inelastic zone is large compared to the length of the cut, $R_I < c$, the large-scale inelasticity prevails, and the work of fracture is independent of the length of the cut and is the same as that of uncut sample.

This discussion brings us to the giant discrepancy in the fractocohesive length between the hydrogel and the perfect network (Fig. 10). For the perfect network, the toughness is estimated by the Lake-Thomas model, $\Gamma_{th} = \phi\sqrt{n}aJ/V$, the work of fracture is estimated by the density of covalent energy, $W_{th} = \phi J/V$, and the fractocohesive length is the same as the end-to-end length of a polymer chain in the undeformed state, $\Gamma/W_f = a\sqrt{n}$, on the order of $\Gamma_{th}/W_{th} \sim 10^{-8}$ m (Chen et al., 2017). For the hydrogel, the toughness is amplified by about two orders of magnitude, and the work of fracture is reduced by a factor about four orders of magnitude, so that the fractocohesive length is amplified by six orders of magnitude, on the order of $\Gamma/W_f \sim 10^{-2}$ m. We have traced this giant discrepancy to network imperfection. For the hydrogel, it is the network imperfection that leads to cut insensitivity.

In the limit of a small crack under the condition of small-scale inelasticity, $R_1 < < c < < H$, the linear elastic fracture mechanics applies. The energy release for cut of length c on the edge of a semi-infinite sample, the energy release rate is (Tada et al., 1973)

$$G = 1.26\pi c\sigma^2/E,$$

where σ is the applied stress and E is Young's modulus. Recall that $W = \sigma^2/2E$ in linear elasticity. Upon rupture, the work of rupture is inversely proportional to the length of the cut:

$$W_f = \frac{\Gamma}{7.9c}.$$

The fractocohesive length, Γ/W_f, is related to an equation introduced in (Thomas, 1955):

$$G = W_f d,$$

where G is the energy release rate, and d is the tip diameter of the cut. Thomas cut samples with cuts of various tip diameters d, and for each sample measured the critical energy release rate G_c for the onset of rupture. He showed that G_c/d was a constant independent of d, and was comparable to the work of fracture measured using an uncut sample, W_f. He then argued that for a sample with a razor cut, there was nevertheless an "effective diameter" of the tip upon rupture. He related this effective diameter to the irregularities developed at the tip of the cut approaching rupture. Thus, his effective diameter is the fractocohesive length Γ/W_f as we use now, where Γ is the toughness measured using a sample congaing a long cut, and W_f is the work of fracture measured using a sample containing no intentional cut. Thomas, however, did not relate his effective diameter to cut sensitivity. For gels and elastomers, the relation between the fractocohesive length and cut sensitivity was first identified in (Chen et al., 2017).

The fractocohesive length is distinct from the elastocapillary length γ/μ, where γ is the surface energy and μ is the elastic modulus. For a polyacrylamide hydrogel, $\gamma \sim 0.1 \mathrm{J/m^2}$ and $\mu \sim 10^3 \mathrm{J/m^3}$, so that $\gamma/\mu \sim 10^{-4}$ m. The elastocapillary length appears in elastocapillary phenomena when both elasticity and capillarity are significant (Liu et al., 2019; Style et al., 2017).

The fractocohesive length is also distinct from the elastocohesive length Γ/E, where E is Young's modulus (Creton and Ciccotti, 2016; Hui et al., 2003). For highly stretchable materials such as the polyacrylamide hydrogels, $\Gamma \sim 10^3\,\mathrm{J/m^2}$, $W_f \sim 10^5\,\mathrm{J/m^3}$, and $E \sim 10^3\,\mathrm{J/m^3}$, so that the elastocohesive length is $\Gamma/E = 1$ m, and is larger than the fractocohesive length by two orders of magnitude. The elastocohesive length scales the size of zone of finite elastic deformation.

8. Concluding remarks

For a polyacrylamide hydrogel, we have shown that experimental measurements map network imperfection to mechanical properties. Compared to a perfect network, the real, imperfect network reduces the work of fracture by four orders of magnitude, amplifies the toughness by two orders of magnitude, and amplifies the fractocohesive length by six orders of magnitude. It is the network imperfection that makes the polyacrylamide hydrogel cut insensitive, the threshold for crack growth under cyclic load much below the toughness, and the threshold for crack growth under cyclic load distinct from that under static load. In studying polymer networks, network imperfection richly deserves our attention, just as fillers, viscoelasticity, and poroelasticity. Network imperfection keeps the ultimate properties within small scatter, but does greatly reduce the ultimate properties relative to those of a perfect network. The large gap between the ultimate properties of the hydrogel and those of a perfect network poses an immediate question: how can we synthesize new hydrogels with much higher ultimate properties?

Acknowledgement

This work at Harvard is supported by the NSF MRSEC (DMR-1420570). T. Yin is supported by the China Scholarship Council as a visiting scholar at Harvard University.

References

Ahagon, A., Gent, A., 1975. Threshold fracture energies for elastomers. J Polymer Sci 13, 1903–1911.
Arruda, E.M., Boyce, M.C., 1993. A three-dimensional constitutive model for the large stretch behavior of rubber elastic materials. J Mech Phys Solids 41, 389–412.
Bai, R., Chen, B., Yang, J., Suo, Z., 2019a. Tearing a hydrogel of complex rheology. J Mech Phys Solids.
Bai, R., Yang, J., Morelle, X.P., Yang, C., Suo, Z., 2018. Fatigue fracture of self-recovery hydrogels. ACS Macro Lett 7, 312–317.
Bai, R., Yang, J., Suo, Z., 2019b. Fatigue of hydrogels. Eur J Mech A/Solids 74, 337–370.
Bai, R., Yang, Q., Tang, J., Morelle, X.P., Vlassak, J., Suo, Z., 2017. Fatigue fracture of tough hydrogels. Extreme Mech Lett 15, 91–96.
Beyer, M.K., 2000. The mechanical strength of a covalent bond calculated by density functional theory. J Chem Phys 112, 7307–7312.
Bueche, F., 1959. The tensile strength of elastomers according to current theories. Rubber Chem. Technol. 32, 1269–1285.
Cai, S., Suo, Z., 2012. Equations of state for ideal elastomeric gels. EPL (Europhysics Letters) 97, 34009.
Caulfield, M.J., Qiao, G.G., Solomon, D.H., 2002. Some aspects of the properties and degradation of polyacrylamides. Chem Rev 102, 3067–3084.
Chen, C., Wang, Z., Suo, Z., 2017. Flaw sensitivity of highly stretchable materials. Extreme Mech Lett 10, 50–57.
Creton, C., Ciccotti, M., 2016. Fracture and adhesion of soft materials: a review. Rep Prog Phys 79, 046601.
Diani, J., Fayolle, B., Gilormini, P., 2009. A review on the Mullins effect. Eur Polym J 45, 601–612.
Dobrynin, A.V., Colby, R.H., Rubinstein, M., 2004. Polyampholytes. J Polym Sci, Part B 42, 3513–3538.
Ducrot, E., Chen, Y., Bulters, M., Sijbesma, R.P., Creton, C., 2014. Toughening elastomers with sacrificial bonds and watching them break. Science 344, 186–189.
Edwards, S., Vilgis, T.A., 1988. The tube model theory of rubber elasticity. Rep Prog Phys 51, 243.
Gent, A., 1996. Adhesion and strength of viscoelastic solids. Is there a relationship between adhesion and bulk properties? Langmuir 12, 4492–4496.
Gong, J.P., Katsuyama, Y., Kurokawa, T., Osada, Y., 2003. Double-network hydrogels with extremely high mechanical strength. Adv. Mater. 15, 1155–1158.
Greensmith, H., 1956. Rupture of rubber. IV. Tear properties of vulcanizates containing carbon black. J Polym Sci 21, 175–187.
Greensmith, H., 1960. Rupture of rubber. VIII. Comparisons of tear and tensile rupture measurements. J Appl Polym Sci 3, 183–193.
Griffith, A.A., 1921. VI. The phenomena of rupture and flow in solids. In: Series A, containing papers of a mathematical or physical character, 221. Philosophical transactions of the royal society of London, pp. 163–198.
Hamed, G., 2007. Rubber reinforcement and its classification. Rubber Chem Technol 80, 533–544.
Hamed, G.R., 1994. Molecular aspects of the fatigue and fracture of rubber. Rubber Chem Technol 67, 529–536.
Hu, Y., Suo, Z., 2012. Viscoelasticity and poroelasticity in elastomeric gels. Acta Mech Solida Sin 25, 441–458.
Hui, C.-Y., Bennison, S., Londono, J., 2003. Crack blunting and the strength of soft elastic solids. Proc R Soc Lon Series A 459, 1489–1516.
Irwin, G., 1948. In: Fracturing of metals, 147. ASM, Cleveland, p. 19. -19.
Kalcioglu, Z.I., Mahmoodian, R., Hu, Y., Suo, Z., Van Vliet, K.J., 2012. From macro-to microscale poroelastic characterization of polymeric hydrogels via indentation. Soft Matter 8, 3393–3398.
Keplinger, C., Sun, J.-Y., Foo, C.C., Rothemund, P., Whitesides, G.M., Suo, Z., 2013. Stretchable, transparent, ionic conductors. Science 341, 984–987.
Kolvin, I., Cohen, G., Fineberg, J., 2018. Topological defects govern crack front motion and facet formation on broken surfaces. Nat Mater 17, 140.
Lake, G., Thomas, A., 1967. The strength of highly elastic materials. Proc R Soc Lon 300, 108–119.
Lee, H.R., Kim, C.C., Sun, J.Y., 2018. Stretchable ionics–a promising candidate for upcoming wearable devices. Adv Mater 30, 1704403.
Liu, Q., Ouchi, T., Jin, L., Hayward, R., Suo, Z., 2019. Elastocapillary Crease. Phys Rev Lett 122, 098003.
Llorente, M., Andrady, A., Mark, J., 1981. Model networks of end-linked polydimethylsiloxane chains. XI. Use of very short network chains to improve ultimate properties. J Polymer Sci 19, 621–630.
Long, R., Hui, C.-Y., 2015. Crack tip fields in soft elastic solids subjected to large quasi-static deformation—a review. Extreme Mech Lett 4, 131–155.
Luo, Y.-R., 2007. Comprehensive handbook of chemical bond energies. CRC press.
Mao, Y., Anand, L., 2018. A theory for fracture of polymeric gels. J Mech Phys Solids 115, 30–53.
Mark, J., 2003. Elastomers with multimodal distributions of network chain lengths. In: Macromolecular symposia. Wiley Online Library, pp. 121–130.

Mark, J.E., 1994. Elastomeric networks with bimodal chain-length distributions. Acc Chem Res 27, 271–278.
Mullins, L., 1948. Effect of stretching on the properties of rubber. Rubber Chem Technol 21, 281–300.
Nakajima, T., Sato, H., Zhao, Y., Kawahara, S., Kurokawa, T., Sugahara, K., Gong, J.P., 2012. A universal molecular stent method to toughen any hydrogels based on double network concept. Adv Funct Mater 22, 4426–4432.
Orowan, E., 1950. Fatigue and fracture of metals. Symposium at massachusetts institute of technology.
Proctor, B., Whitney, I., Johnson, J., 1967. The strength of fused silica. Proc R Soc Lond Series A 297, 534–557.
Rivlin, R., Thomas, A.G., 1953. Rupture of rubber. I. Characteristic energy for tearing. J Polym Sci 10, 291–318.
Sato, K., Nakajima, T., Hisamatsu, T., Nonoyama, T., Kurokawa, T., Gong, J.P., 2015. Phase-separation-induced anomalous stiffening, toughening, and self-healing of polyacrylamide gels. Adv Mater 27, 6990–6998.
Smith, T.L., 1978. Strength of elastomers. A perspective. Rubber Chem Technol 51, 225–252.
Style, R.W., Jagota, A., Hui, C.-Y., Dufresne, E.R., 2017. Elastocapillarity: surface tension and the mechanics of soft solids. Ann Rev Condensed Matter Phys 8, 99–118.
Sun, J.-Y., Zhao, X., Illeperuma, W.R., Chaudhuri, O., Oh, K.H., Mooney, D.J., Vlassak, J.J., Suo, Z., 2012. Highly stretchable and tough hydrogels. Nature 489, 133.
Tada, H., Paris, P.C., Irwin, G.R., 1973. The stress analysis of cracks. handbook. Del Research Corporation.
Tanaka, Y., Fukao, K., Miyamoto, Y., 2000. Fracture energy of gels. Eur Phys J E 3, 395–401.
Tang, J., Li, J., Vlassak, J.J., Suo, Z., 2017. Fatigue fracture of hydrogels. Extreme Mech Lett 10, 24–31.
Tehrani, M., Sarvestani, A., 2017. Effect of chain length distribution on mechanical behavior of polymeric networks. Eur Polym J 87, 136–146.
Thomas, A., 1955. Rupture of rubber. II. The strain concentration at an incision. J Polym Sci 18, 177–188.
Thomas, A., 1958. Rupture of rubber. V. Cut growth in natural rubber vulcanizates. J Polym Sci 31, 467–480.
Tian, K., Bae, J., Suo, Z., Vlassak, J.J., 2018. Adhesion between hydrophobic elastomer and hydrogel through hydrophilic modification and interfacial segregation. ACS Appl Mater Interfaces 10, 43252–43261.
Wang, Z., Xiang, C., Yao, X., Le Floch, P., Mendez, J., Suo, Z., 2019. Stretchable materials of high toughness and low hysteresis. Proceedings of the National Academy of Sciences.
Webber, R.E., Creton, C., Brown, H.R., Gong, J.P., 2007. Large strain hysteresis and mullins effect of tough double-network hydrogels. MacromoleculesMacromolecules 40, 2919–2927.
Yang, C., Suo, Z., 2018. Hydrogel ionotronics. Nat Rev Mater 3, 123–142.
Yang, C.H., Wang, M.X., Haider, H., Yang, J.H., Sun, J.-Y., Chen, Y.M., Zhou, J., Suo, Z., 2013. Strengthening alginate/polyacrylamide hydrogels using various multivalent cations. ACS Appl Mater Interfaces 5, 10418–10422.
Zhang, E., Bai, R., Morelle, X.P., Suo, Z., 2018. Fatigue fracture of nearly elastic hydrogels. Soft Matter 14, 3563–3571.
Zhong, M., Wang, R., Kawamoto, K., Olsen, B.D., Johnson, J.A., 2016. Quantifying the impact of molecular defects on polymer network elasticity. Science 353, 1264–1268.